Biogeosciences Discuss., 11, 9813–9852, 2014
www.biogeosciences-discuss.net/11/9813/2014/
doi:10.5194/bgd-11-9813-2014

Biogeosciences Discussions
Open Access

Methane related changes in prokaryotic activity along geochemical profiles in sediments of Lake Kinneret (Israel)

I. Bar Or[1], E. Ben-Dov[2,3], A. Kushmaro[2,5,6], W. Eckert[4], and O. Sivan[1]

[1]Department of Geological and Environmental Sciences, Ben-Gurion University of the Negev, Be'er-Sheva, P.O. Box 653, 8410501, Israel
[2]Avram and Stella Goldstein-Goren Department of Biotechnology Engineering, Ben-Gurion University of the Negev, Be'er-Sheva, P.O. Box 653, 8410501, Israel
[3]Department of Life Sciences, Achva Academic College, Achva, M.P. Shikmim 79800, Israel
[4]Israel Oceanographic and Limnological Research, The Yigal Allon Laboratory, P.O. Box 447, 14950 Migdal, Israel
[5]National Institute for Biotechnology in the Negev, Ben-Gurion University of the Negev, P.O. Box 653, Beer-Sheva 8410501, Israel
[6]School of Materials Science and Engineering, Nanyang Technological University, Singapore

Received: 27 May 2014 – Accepted: 5 June 2014 – Published: 24 June 2014

Correspondence to: A. Kushmaro (arielkus@bgu.ac.il)

Published by Copernicus Publications on behalf of the European Geosciences Union.

Abstract

Microbial methane oxidation process (methanotrophy) is the primary control on the emission of the greenhouse gas methane (CH_4) to the atmosphere. In terrestrial environments, aerobic methanotrophic bacteria are mainly responsible for oxidizing the methane. In marine sediments the coupling of the anaerobic oxidation of methane (AOM) with sulfate reduction, often by a consortium of anaerobic methanotrophic archaea (ANME) and sulfate reducing bacteria, was found to consume almost all the upward diffusing methane. Recently, we showed geochemical evidence for AOM driven by iron reduction in Lake Kinneret (LK) (Israel) deep sediments and suggested that this process can be an important global methane sink. The goal of the present study was to link the geochemical gradients found in the porewater (chemical and isotope profiles) with possible changes in microbial community structure. Specifically, we examined the possible shift in the microbial community in the deep iron-driven AOM zone and its similarity to known sulfate driven AOM populations. Screening of archaeal 16S rRNA gene sequences revealed *Thaumarchaeota* and *Euryarchaeota* as the dominant phyla in the sediment. *Thaumarchaeota*, which belongs to the family of copper containing membrane-bound monooxgenases, increased with depth while *Euryarchaeota* decreased. This may indicate the involvement of *Thaumarchaeota*, which were discovered to be ammonia oxidizers but whose activity could also be linked to methane, in AOM in the deep sediment. ANMEs sequences were not found in the clone libraries, suggesting that iron-driven AOM is not through sulfate. Bacterial 16S rRNA sequences displayed shifts in community diversity with depth. *Proteobacteria* and *Chloroflexi* increased with depth, which could be connected with their different dissimilatory anaerobic processes. The observed changes in microbial community structure suggest possible direct and indirect mechanisms for iron-driven AOM in deep sediments.

BGD
11, 9813–9852, 2014

1 Introduction

Chemical profiles in the porewater of aquatic sediments reflect the sequence of microbial mediated redox reactions that are driven by the availability both of organic matter as an energy source and of suitable electron acceptors. The latter are depleted in the order of decreasing chemical potential, beginning with oxygen and proceeding through nitrate, manganese and iron oxides, and then sulfate. Below the main zone of sulfate reduction, the fermentation of organic carbon leads to the formation of methane (CH_4) by the process of methanogenesis (Froelich et al., 1979).

The methane produced is isotopically depleted in ^{13}C, with values of ~ -50 to -110 ‰ (Schoell, 1988), and the residual dissolved inorganic carbon (DIC) pool is enriched by an isotopic fractionation factor (ε) of 50 to 70 ‰ (e.g., Borowski et al., 2000; Whiticar, 1999). When the produced methane diffuses into contact with an available electron acceptor, it can be consumed by microbial oxidation (methanotrophy), the main process by which the important greenhouse methane is prevented from escaping into the atmosphere. In the terrestrial environment, bacteria are mainly responsible for oxidizing methane to CO_2 using O_2 as the electron acceptor (Chistoserdova et al., 2005). In marine sediments, where its mainly anaerobic environments, archaea are found to consume the majority of upward diffusing methane coupled to sulfate reduction (Knittel and Boetius, 2009; Thauer, 2010; Valentine, 2002).

Evidence from lipids and from fluorescence in situ hybridization (FISH) showed that a consortium of archaea and sulfate reducing bacteria are involved in this anaerobic methane oxidation (AOM) (Boetius et al., 2000; Hinrichs et al., 1999; Orphan et al., 2001). To date, three groups of anaerobic methanotrophic archaea (ANME), named ANME-1, ANME-2, and ANME-3, are known to perform sulfate driven AOM (Niemann et al., 2006; Orphan et al., 2002). However Milucka et al. (2012) demonstrated AOM mediated solely by archaea, where the archaea was shown to oxidize the methane and reduce the sulfate to elemental sulfur. Disproportionating bacteria, also involved in this mechanism, oxidize and reduce this elemental sulfur to sulfate and sulfide, respectively.

BGD
11, 9813–9852, 2014

The carbon isotopic fractionation factor (ε) for this methanotrophic process was shown to be in the range of 4–30 ‰ (Kinnaman et al., 2007; Whiticar, 1999). Enrichment cultures of ANME from different environments showed a carbon isotopic fractionation of 12–39 ‰ (Holler et al., 2009).

Other electron acceptors were recently shown to drive AOM. Nitrite driven AOM by oxygenic bacteria was observed in two different freshwater ecosystems in the Netherlands (Ettwig et al., 2009; Raghoebarsing et al., 2006) and in peatlands (Zhu et al., 2012). Beal et al. (Beal et al., 2009) showed the potential of manganese and iron-driven AOM in marine sediments. In our recent study (Sivan et al., 2011), we provided in situ geochemical evidence for AOM coupled to microbial iron reduction, which occurs below the main methanogenesis zone in Lake Kinneret (LK) sediments where dissolved sulfate and nitrate are no longer available.

The changes with depth in available electron acceptors and in type of organic material coincide with microbial community shifts. Combined geochemical gradients found in the porewater (chemical and isotope profiles) and prokaryotic sediment profiles, therefore, can shed light on the mechanisms of the microbial processes involved in AOM in LK sediments. This study comprised a microbial survey of the sediment depths in LK based on the main electron acceptors at the different depths to track the microbial system involved in the methane cycle in this environment. Specifically, the study examined the possible shift in the microbial communities in the deep iron-driven AOM zone and their similarities to known sulfate driven AOM populations.

2 Material and methods

2.1 Study site

Located in northern Israel, Lake Kinneret (LK, Fig. 1) is a warm monomictic subtropical lake. Typical concentrations of major electron acceptors in the water column during the mixed period are 35–50 µM nitrate and 600 µM sulfate (Adler et al., 2011; Serruya

BGD
11, 9813–9852, 2014

et al., 1974). In the spring, the newly formed epilimnion is characterized by increasing temperatures and enhanced phytoplankton development, while in the hypolimnion heterotrophic microorganisms gradually deplete oxygen and then nitrate. Organic matter degradation by bacterial iron and manganese reduction takes place below the thermocline in the summer. At the end of the stratification period, sulfate reduction occurs in the bottom water. In the upper part of the sediment, sulfate reduction is the dominant microbial process year round, and below depths of 5 cm sulfate reduction processes are mainly replaced by methanogenesis (Adler et al., 2011; Eckert and Conrad, 2007). Total iron content ($Fe_{(tot)}$) is around 3 % in the upper 40 cm of the sediment (Eckert, 2000) and the manganese concentration is about 700 µg g^{-1} (Serruya, 1971). The organic matter carbon content is about 3 % (dry weight) at the top and decreases to 2 % at a depth of 40 cm (Serruya, 1978).

2.2 Sampling

Sediment cores were collected from the center of the lake (Station A, Fig. 1) at a water depth of ~ 42 m (maximum lake water column depth) at different times using Perspex tubes, measuring 55 cm long by 5 cm in diameter, with a gravity corer. The cores were stored in the dark at 4 °C until they were sliced later on the same day or the day after. Core sampling for the microbial community study took place in December 2009. The methane profile presented was taken two weeks before this sampling for the microbial communities (also December 2009). The $\delta^{13}C_{CH_4}$ and $\delta^{56}Fe$ profiles were performed four months before the microbial sampling (August 2009). Sampling for Fe(II), Mn(II) and SO_4^{-2} profiles was done from 2007 to 2011 and that for sulfide is from June 2013 (sulfide profiles from 2007 are presented in Sivan et al., 2011). Over a dozen porewater chemical and isotope profiles were generated seasonally from 2007 to 2013. The slight seasonal changes we found allowed us to use typical geochemical profiles (shown here) in order to sample for the microbiology communities in the different electron ac-

BGD
11, 9813–9852, 2014

ceptors zones and to correlate between the microbial sampling and the geochemical profiles.

2.3 Geochemical analyses

Cores were cut into 2 cm slices under a constant flow of N_2 using a slicing device. About 1.5 mL of each sediment slice was transferred into N_2-flushed crimp bottles containing 5 mL of 1.5 N NaOH for the headspace measurements of CH_4 and $\delta^{13}C_{CH_4}$ (after Sivan et al., 2011). CH_4 concentrations were measured on a SHIMADZU gas chromatograph equipped with a FID detector at a precision of 2 µmol L^{-1}.

Porewater was extracted immediately from each slice by centrifugation at 27 000 g at 4 °C in a N_2 atmosphere, and the supernatant was filtered through 0.45 µm filters. A 1 mL subsample was fixed with Ferrozine and analyzed for dissolved Fe(II) (Stookey, 1970). Four millimeters of subsample were poured into an acidified vial (1 mL of 0.5N nitric acid) to measure dissolved manganese. The sample was analyzed via an Inductively Coupled Plasma Mass Spectrometer (ICP-MS, Elan DRC II, Perkin Elmer) at a precision of ±10 %. For sulfide profiles, 1 mL of subsample was added to zinc acetate and hydrogen sulfide concentrations were determined by the methylene blue method (Cline, 1969). For sulfate measurements, 5 mL of subsample were analyzed with a Dionex DX500 high pressure liquid chromatograph with a precision of ±3 %. Iron isotope analysis was done by acidifying the subsamples with 10 % HCl for one week (to dissolve any precipitated iron) and then purifying them by anion exchange chromatography (Borrok et al., 2007). δ^{56}Fe was measured on a Neptune multi-collector ICP-MS in high resolution mode according to standard methods and standardized against isotopic reference material (IRMM-014) with a precision of ±0.1 ‰ (John and Adkins, 2010). Total lipids were extracted using the Bligh–Dyer procedure (Bligh and Dyer, 1959) with solvent mixture of 2 : 1 : 0.8 (methanol : dichloromethane : buffer). $\delta^{13}C$ of the total lipid extraction (TLE) was measured on an Elemental Analyzer Isotopic Ratio Mass Spectrometer (EA-IRMS) with a precision of 0.1 %.

BGD
11, 9813–9852, 2014

2.4 DNA extraction and amplification from sediment samples

Some of the sediment slices were kept frozen for the microbial work. Samples from three different depths (0–3 cm representing the sulfate reduction zone, 6–9 cm representing the methanogenesis zone, and 29–32 cm representing the deep AOM zone) were defrosted. Total genomic DNA was extracted from the sediment samples using the MoBio Power Soil DNA isolation kit (MoBio Laboratories, Solana Beach, CA). Genomic DNA was eluted using 60 µL of elution buffer and stored at −20 °C. Concentrations of DNA were determined via UV-Vis spectrophotometry (ND-1000 NanoDrop Technologies, Wilmington, DE) (sulfate reduction zone 22 ng μL^{-1}, methanogenesis zone 35.8 ng μL^{-1} and AOM zone 14 ng/µL).

16S rRNA gene fragments were amplified by PCR using a Biometra T Gradient thermocycler (Biometra, Göttingen, Germany) with the common universal bacterial primer pair (8F, 907R) (Ben-Dov et al., 2006) and universal archaeal pair (21F, 915R) (DeLong, 1992; Stahl and Amann, 1991) targeting 16S rRNA genes. All primer sets were used in PCR amplifications in parallel with Dream Taq (PCR Master mix containing 1.5 mM $MgCl_2$ and a 0.2 mM concentration of each deoxynucleoside triphosphate) (Fermentas, Litvania). An initial denaturizing step of 4 min at 95 °C was followed by 30 cycles of the following incubation pattern: 94 °C for 30 s, 54 °C for 30 s, and 72 °C for 60–90 s. A final extension at 72 °C for 20 min completed the reaction.

2.5 Clone library construction and sequencing

Polymerase chain reaction (PCR) products were purified by electrophoresis via a 0.8 % agarose gel (Sigma) stained with ethidium bromide and visualized on a UV transilluminator. The amplified 16S rRNA gene bands were excised from the gel and the DNA was purified from the gel slice using the Wizard PCR Prep kit (Promega, Madison, Wis.). The gel-purified PCR products were cloned into the pCRII-TOPO-TA cloning vector as specified by Invitrogen (Carlsbad, CA) and transformed into calcium chloride-competent HD5*α* *E. coli* cells according to the manufacturer's instructions and stan-

BGD
11, 9813–9852, 2014

dard techniques. The transformed cells were spread onto an LB agar medium. White colonies harboring plasmids with inserts were used for amplification of the inserts with M13-F and M13-R primers annealing to the plasmid. Sequencing was performed by an ABI PRISM dye terminator cycle sequencing ready reaction kit with an AmpliTaq DNA polymerase FS and DNA sequencer ABI model 373A system (Perkin–Elmer).

2.6 Sequence analysis

Sequences were first screened for chimeras using the Bellerophon server (Huber et al., 2004). An additional chimera check was then run by manually cutting sequences in half and aligning them with the ARB database (Ludwig et al., 2004). When the two halves did not align, the original sequence was considered to be a chimera sequence. In this study, all 16S rRNA gene sequences were phylogenetically classified by the SINA classifier program (Pruesse et al., 2012) with $\geq 70\,\%$ similarity. Sequences that were unidentified by SINA were aligned in ARB (Ludwig et al., 2004) and were classified to phyla according to their alignment within the ARB phylogenetic database. In addition, sequences were grouped into operational taxonomic units (OTUs) on the basis of rRNA gene sequences of 97 % similarity using different programs. First, a distance matrix was generated using the MEGA5 package (Tamura et al., 2011). This matrix was then fed into the DOTUR computer program with all default options (Schloss and Handelsman, 2005). Diversity indexes (Chao and Ace) were calculated by Dotur, and the homologous coverage (biodiversity coverage) C was determined using the following equation: $C = 1 - (N/n)$, where N is the number of phylotypes and n is the total number of analyzed clones (Good, 1953). The Morisita–Horn similarity index (Magurran, 1988) was calculated using the EstimateS statistical program, software version 8.1 (Colwell et al., 2012). All of the sequences and their closest relative matches with similarity of $> 96\,\%$ to uncultured and $> 90\,\%$ to cultured microbial sequences were obtained from NCBI BLAST and were aligned using the MEGA5 package (Tamura et al., 2011). Neighbor-joining phylogenetic trees were created using the MEGA5 package. The rel-

BGD
11, 9813–9852, 2014

ative confidence of the tree topologies was evaluated by performing 1000 boot-strap replicates.

2.7 Nucleotide sequence accession numbers

The nucleotide sequences obtained in this study were deposited in the NCBI GenBank database under accession numbers HQ636112–HQ636255 for the bacterial 16S rRNA genes and HQ636257–HQ636418 for the archaeal 16S rRNA genes.

3 Results

3.1 Porewater profiles

This study focused on microbial community shifts along porewater profiles of electron acceptor gradients related to the methane cycle in porewater profiles. Over dozen of geochemical profiles of the porewater at station A (Fig. 1) were performed seasonally to characterize shifts in main electron acceptors with depth. The profiles shown (Fig. 2) are typical representatives of the geochemical seasonal profiles of The similarities between samples at all depths indicate only slight seasonal changes (Adler et al., 2011; Sivan et al., 2011). Based on these profiles, we divided the sediment into three main redox zones and their corresponding microbial populations.

Oxygen and nitrate during the stratified period of the lake (when the sediment was collected for this work) were already depleted in the water column below the thermocline. Even during the mixing period of the lake, oxygen was completely depleted in the sediment below depths of 0.4 cm and nitrate was not detected (Eckert et al., 2002). Sulfate reduction was the main process in the upper few centimeters of the sediment throughout the year (Eckert and Conrad, 2007; Hadas and Pinkas, 1992), and in the upper 15 cm of sediment, sulfate was depleted during both the stratified and the mixed periods of the lake. The typical concave-down curvature of the profiles of sulfate and sulfide in porewater up to its depletion around 15 cm depth (Fig. 2c) suggests bacterial

BGD
11, 9813–9852, 2014

utilization of the sulfate. A typical LK methane concentration profile (Fig. 2a) shows that methane concentrations increased from 250 µM at the water–sediment interface to a maximum of about 1.5 mM in the depth range of 7 to 15 cm. The methane concentration was usually decreased below 15 cm depth, suggesting its oxidation in the deep sediments. The profile of $\delta^{13}C_{CH_4}$ (Fig. 2a) showed a decrease from −60 ‰ at a depth of 1 cm to about −65 ‰ at a depth of 7 cm and then an increase in the deeper sediments to a maximum value of −53.5 ‰ at a depth of 25 cm. Also, the profile of $\delta^{13}C_{TLE}$ (Fig. 2d) showed that it decreased in the deepest part of the sediment, implying the production of biomass from a light source.

These profiles results suggest that below depths of about 20 cm (below the methanogenesis peak) there is a methane sink coupled to electron acceptors other than dissolved sulfate and nitrate, which are depleted at such depths. Thus, the most probable electron acceptors are manganese and iron oxides. Indeed, the dissolved Mn(II) concentration (Fig. 2b) increased from 5 µM at the top of the sediment to a plateau of about 23 µM from depths of 23 to 36 cm. Although the Fe(II) concentration profile also showed an increase with depth (Fig. 2b), that occurred in a manner that differed from that of the manganese profile. In the upper 15 cm, dissolved Fe(II) concentrations were below the detection limit. Dissolved Fe(II) probably reacted with sulfide and precipitated as iron sulfide minerals in the sulfide zone, but then gradually increased below 15 cm to about 90 µM at a depth of 36 cm. This dramatic increase in Fe(II) below the sulfate zone suggests the involvement of Fe(III) reduction to Fe(II) in the deep sediments. Mild acid extractions of highly reactive iron minerals in the sediment yielded at least 40 µmol g dry wt^{-1} sediment of easily accessible Fe(III) throughout the sediments, which can support the amount of iron reduction observed to occur in the sediment. Moreover, the δ^{56}Fe profile (Fig. 2d) was also consistent with active Fe(III) reduction (Sivan et al., 2011). The precipitation of ferrous iron with sulfides would cause heavier values in the dissolved isotopic δ^{56}Fe (Butler et al., 2005), as was shown in the upper sediments. However, in the zone of apparent AOM, the δ^{56}Fe values were lighter (−1.7 % to −2.3 %) than in the upper part of the sediment and similar to those ob-

BGD
11, 9813–9852, 2014

served in active Fe(III) reduction zones in porewater (Severmann et al., 2006). This iron-driven AOM process was further confirmed by a set of incubation experiments on LK cores [23]. Our model calculations suggest maximum sulfate reduction rates at the water sediment interface of $1.4 \times 10^{-12} \pm 0.2 \times 10^{-12}$ mol cm^{-3} s^{-1}, maximum methanogenesis rates at 5–12 cm of $2.5 \times 10^{-13} \pm 1.5 \times 10^{-13}$ mol cm^{-3} s^{-1} and AOM rates below 20 cm of $5 \times 10^{-14} \pm 1 \times 10^{-14}$ mol cm^{-3} s^{-1} (Adler et al., 2011).

3.2 Sediment microbial communities

To study sediment-depth-dependent microbial community shifts, 16S rRNA gene sequences of the prokaryotic community from three different depth zones (0–3, 6–9 and 29–32 cm, see arrows in Fig. 2a) were extracted and analyzed. Those depth zones were chosen based on the geochemical profiles and the geochemical experiments on sediments sampled at different times, which support this division (partly described in (Sivan et al., 2011)). Therefore, microbial community sampling of the three depth zones at a single time point should represent the different microbial habitats as they pertain to the respective geochemical zones. The diverse bacterial and archaeal communities at these depth zones varied in composition and richness throughout the sediment. A total of 127 and 153 bacterial and archaeal sequences representing 85 and 112 OTUs (cut-off value of 97 %), respectively, were identified. Estimates of phylotype richness, diversity coverage and similarity were calculated according to the abundance-based coverage estimate (ACE), Chao's estimator (Chao, 1984; Chao and Ma, 1993), the Shannon diversity index, Good's coverage and the Morisita–Horn similarity index (Tables 1 and 2, Supplementary Tables S1 and S2). Because clone library coverage shows that the microbial communities in the sediment were not fully sampled, the sequences percentages in the libraries are only rough estimations instead of actual relative community percentages in this environment.

All the estimators indicated a high degree of richness in the bacteria communities throughout all of the sediments (Table 1). The highest bacterial richness calculated was at depths of 6–9 cm. However, the bacterial coverage (Good, 1953) estimations

BGD
11, 9813–9852, 2014

(~ 26 % coverage) showed that sediment depth intervals were not completely sampled, and therefore, they failed to capture the total estimated richness and diversity at each depth (Table 1). The Shannon index and richness estimators (Chao and Ace) returned high values that were higher than those for archaea (Table 2), indicating a highly diverse community.

Most of the sequences of LK were very similar to those of uncultured environmental microorganisms retrieved from freshwater lakes. About 62 % of the bacterial sequences in the upper 10 cm of the sediment were more than 90 % similar to sequences from previous studies conducted in LK (Nüsslein et al., 2001; Schwarz et al., 2007a, b). The bacterial diversity and richness in the sediment show much more complex communities than those of the archaea, which complicated estimating the functionality of those microorganisms. Our Shannon index values (3.19–3.94) in the bacteria are lower than those of previous studies (Schwarz et al., 2007a; Wobus et al., 2003) as a result of the low coverage of the communities in the sample. Yet the abundant communities were probably still represented in the clone libraries.

Although the bacterial OTUs were distributed over 21 phyla, only *Proteobacteria*, *Chloroflexi, Nitrospirae*, *Bacteroidetes* and *Planctomycetes* were over 10 % in one of the clone libraries (Fig. 3a). The percentages in the clone libraries of the two dominant phyla members, *Proteobacteria* and *Chloroflexi*, increased with depth: *Proteobacteria* from 25 % to 34 % and *Chloroflexi* from 16 % to 29 %. The *Nitrospirae* phylum was not detected in the upper part of the sediment, but in the bottom section they were found at a relatively high percentage (~ 11 %). The rest of the phyla showed different and variable patterns.

When focusing on the classes of all the bacterial sequences, the phylogenetic linage of the dominant phyla exhibits a distinctive pattern (Fig. 3b). From the *Proteobacteria*, the *Gammaproteobacteria* increased with depth while *Deltaproteobacteria* were found at the same percentage in the clone libraries throughout the sediment. Alpha, Beta and *Epsilonproteobacteria* were recovered from at least one sample, but at different depths. In the *Chloroflexi* phyla, *Caldilineae* and *Anaerolineae* showed approximately

BGD
11, 9813–9852, 2014

the same percentages throughout the two lower samples. The *Nitrospirae* phyla in the middle sample were divided between OPB95 and *Nitrospiraceae*, and in the lower part only *Nitrospira* were found. The bacterial phylogenetic tree from the deep part of the sediment (Fig. 5a) showed that *Gammaproteobacteria* sequences were similar to sequences that have already been found in LK and to aerobic methanotrophic bacteria. Our *Deltaproteobacteria* sequences were similar to those found in varied environments, which include iron reducing bacteria. The sequences of the *Chloroflexi* phylum comprised a few close reference sequences that are mostly unknown. In our clone library, the *Nitrospirae* phylum had one sequence closely affiliated with bacteria investigated in the degradation of phenanthrene and pyrene in freshwater sediments in a fuel cell environment with added amorphous ferric hydroxide (Zheng et al., 2014).

The bacterial Morisita–Horn similarity index (Table S1) together with the Venn diagram (Fig. S1) showed low correlation between the different depths. Only two OTUs were shared between the upper and lower sections, while five were shared in the middle and lower sections. No overlap was detected between the upper and the middle sections of the sediment.

Archaeal coverage estimations of about 65 % (Table 2) indicated a much higher sampling coverage than for the bacterial communities. The Shannon index and richness estimators (Chao and Ace), which showed lower values than the bacterial indexes at all depths, indicated less diversity. The diversity and richness in the middle section was only slightly higher than in the other parts, despite the gaps in the sampling record (Table 2).

The archaeal 16S rRNA gene sequences (Fig. 4a) were mostly affiliated with the *Euryarchaeota* or *Thaumarchaeota* phyla while *Crenarchaeota* were found in the upper and lower parts of the sediment at low percentages. About 17 % of the sequences in the clone libraries, unclassified by SINA, were instead classified by ARB similarity at the phylum level. *Euryarchaeota* was found to be the dominant phylum, but its percentage decreased with depth (from 80 % to 54 %), while the sequences belonging to *Thaumarchaeota* increased (from 15 % to 43 %). *Thaumarchaeota* sequences were classified

BGD
11, 9813–9852, 2014

into five different classes (Fig. 4b): miscellaneous Crenarchaeotic Group (MCG), which was the dominant class (13 % to 40 % from the top to bottom part respectively), Soil Crenarchaeotic Group (SCG) at a low percentage in the upper part, Marine Benthic Group B (MBG-B) at low percentages in the upper and middle parts, Group C3 at a low percentage in the middle part, and AK59 at a low percentage in the deep part.

Euryarchaeota was mostly divided between *Thermoplasmata*, which was the dominant class (78 % at the top to 51 % at the bottom), *Methanomicrobia* at a low percentage in the upper part, and *Halobacteria* at low percentages in the middle and bottom parts. No ANME sequences were detected even though specific primers (ANME2C-AR468F, ANME3-1249, ANME1-395F, ANME1-1417, ANME3-140F, ANME3-1249, ANME2a-426 and ANME2a-1242R) were tried (Miyashita et al., 2009). The archaeal phylogenetic tree for the deep part of the sediment (Fig. 5b) also shows that representative ANME (AB461389-AB461393) sequences are not close related to any of our sequences. In addition, different levels of classification and similar reference sequences from different environments are shown. *Euryarchaeota* sequences affiliated to our sequences show that they are found in very diverse environments. In contrast, the environments typical for *Thaumarchaeota* representatives associated with our sequences are associated to the methane cycle.

The archaeal Morisita–Horn similarity index for the different depths (Table S2) showed that the communities in the upper and middle parts of the sediment were highly similar, but between the upper and bottom parts the level of similarity declined. However, the numbers of shared OTUs shown by Venn diagram (Fig. S2) between the different depths were limited (only five OTUs overlapped between all the depths), and half of the OTUs at the different depths were not shared. No archaeal 16S rRNA sequence clustering was observed, and no distinct group was formed at any depth. Most of the best matched sequences were from lake sediment environments while some others were also related to environments enriched with sulfur, iron and nitrogen compounds.

BGD
11, 9813–9852, 2014

4 Discussion

In this study of LK sediments we investigated changes in microbial diversity associated with porewater geochemistry and the transition of the dominant electron acceptors with depth (0–40 cm). The geochemical porewater profiles in LK (Fig. 2) suggest that the sediment can be roughly divided to three different regimes of microbial processes: the upper 5 cm dominated by sulfate reduction, the methanogenesis zone between 5 to 17 cm, and the deepest sediments, which are dominated by the anaerobic oxidation of methane coupled to iron reduction. This division of the sediment and the deep iron-driven AOM process were confirmed by in situ profiles of methane, $\delta^{13}C_{CH_4}$, sulfate, and ferrous and subsequent use of a numerical mass conservation model (based on the geochemical profiles of DIC and $\delta^{13}C_{DIC}$ (Adler et al., 2011)) and a set of geochemical incubation experiments conducted in our previous work (Sivan et al., 2011).

The mechanisms that enable the novel process of AOM via iron reduction could be tracked by the existing prokaryotic population at this depth and its resemble to similar environments with a distinct characterization. The size of the clone libraries cannot fully represent the prokaryotic diversity at the different depths. As shown by the coverage, the sequences represent the major communities in the different depth zones. Therefore, calculations of the diversity index and comparisons of the sequences between the different zones can then be related to earlier studies in LK and similar environments as additional tools to interpret the relations between the prokaryotes and the geochemical processes. There are few studies which had analyzed microbial communities relative to geochemical zones in fresh water sediments. Therefor this study deepens the knowledge about microbial communities shift in different electron acceptors conditions, especially that related to methane cycle.

Proteobacteria and *Chloroflexi* were the most abundant bacterial phyla in LK and represented diverse functional groups that increased with depth. *Proteobacteria* is also among the abundant phyla (Schwarz et al., 2007a) in other freshwater sediments (Tamaki et al., 2005; Wobus et al., 2003). Several large classes of *Proteobacteria*

BGD
11, 9813–9852, 2014

were observed, among which *Deltaproteobacteria* were the most abundant (~ 20 %) throughout all sediment samples. They were aligned to strictly anaerobic and sulfate reducing organisms (*Desulfobacteraceae* and *Syntrophobacteraceae*), some of which have been found in iron rich environments. Schwarz et al. (2007a) showed in the upper part of LK that *Deltaproteobacteria* was one of the dominant classes, most of which were affiliated with acetate oxidizing sulfate reducing bacteria, which outcompete the acetoclastic methanogens.

The second abundant phylum was *Chloroflexi*, which also increased with depth and whose most abundant class was *Anaerolineae*, which although found in a variety of anaerobic environments, only a few representatives have been cultivated so far (Yamada and Sekiguchi, 2009). The metabolisms of those representatives showed that they utilized organic matter, but no specific electron acceptor was found (Yamada et al., 2006). Because *Chloroflexi* members were found throughout the entire core, *Anaerolineae* representatives could be the main organic matter decomposers in LK.

Sequences of *Bacteroidetes* were only retrieved in the upper part (0–3 cm) of the LK sediment core, which confirms similar findings by Schwarz et al. (2007a). Known as hydrolytic fermentative bacteria, they are major utilizers of high-molecular-mass dissolved organic matter in marine ecosystems (Cottrell and Kirchman, 2000). Their presence in the upper part of the sediment, therefore, was correlated with their metabolic preference, as they can utilize the fresh organic matter that descents from the water column. It should be noted that the upper sediment may contain denitrifying bacteria that arrived from the water column.

Archaeal communities are responsible for many environmental processes. In LK, archaeal communities represent a small percentage of the prokaryotic communities (Schwarz et al., 2007a), their community compositions changed with depth and their diversity was very high compared to the findings of other studies (e.g., Lehours et al., 2007 in Lake Pavin sediment, Hansel et al., 2008 in a soil profile from the vadoze zone, and Siboni et al., 2008 in corals). However, the similarity index showed a strong resemblance between the different depths at the higher phylogenetic order (phyla and

BGD
11, 9813–9852, 2014

class). Nevertheless, it should be noted that at the OTU level, there was a small overlap and a large difference between the depths (S1).

About 35 % of the archaeal sequences were similar (cut-off 90 %) to those found in previous studies conducted in LK (Nüsslein et al., 2001; Schwarz et al., 2007a, b). The dominant archaeal phylum was *Euryarchaeota* (~ 80 %), which decreased with depth. Among the *Euryarchaeota*, the majority were *Thermoplasmata* (97 %), which included 16S rRNA sequences of the *Thermoplasmatales* order. The MBG-D clade was affiliated with the order *Thermoplasmatales* and was also detected in our libraries. Members of the MBG-D have been shown to exist in a variety of freshwater and marine environments (Beal et al., 2009; Borrel et al., 2012), and it is the most widely encountered, uncultured lineage in freshwater lake sediments. Even though their metabolism is unknown, hypotheses about their functionalities are based on the environments in which they were found. Methanogenesis was suggested, as they were found in deep lake sediments with high methane concentrations (Borrel et al., 2012), and they were also hypothesized to be involved in AOM, as they were found in AOM zones (Schubert et al., 2011) and in marine seep sediment (Beal et al., 2009). However, in other environments, in which methane concentrations were low, the utilization of waste products, intermediates, or dead cells by MBG-D was also suggested (Smith et al., 1975). Recently, a single cell genomics study showed that members of MBG-D were capable of exogenous protein degradation in cold anoxic environments (Lloyd et al., 2013). The other archaeal phyla were *Thaumarchaeota*, which increased with depth, and *Crenarchaeota*, whose representation in the clone library was very low. *Thaumarchaeota* has a specific functionality (see below) while that of *Crenarchaeota* is for the most part unknown.

In the upper layer of sediment (0–3 cm), sulfate concentrations are the highest and are gradually consumed with depth (Hadas and Pinkas, 1992) as particulate organic matter from the water column accumulates, making organic carbon degradation available. Adler et al. (2011) calculated that the bulk of bacterial sulfate reduction occurs in the top 1 cm of sediment, a finding that was supported by the microbial work of Hadas

BGD
11, 9813–9852, 2014

et al. (1992). Using sulfide and particulate organic carbon measurements, Eckert and Conrad (2007) also showed that sulfate reduction accounts for most of the mineralization of organic matter in the upper 15 cm of sediment. Methane concentrations in the upper layer are relatively low and mainly come from diffusion as methanogens are outcompeted by sulfate reducers (Lovley and Klug, 1983). The depletion in methane concentrations and declining $\delta^{13}C_{TLE}$ values and the heavier isotopic values of $\delta^{13}C_{CH_4}$ in the upper layer compared to the methanogenic zone may be explained by AOM via sulfate reduction, although no ANME sequences were found using specific primers or by phylogenetic alignment (Fig. 5b) at any depth in the sediment. Our finding in this depth of the lowest bacterial diversity between the sediment depths could be caused by the dominant bacterial communities, which utilized the easily degradable organic substrates coming from the water column with the available electron acceptors.

In the middle layer of sediment (6–9 cm), methane production was the highest (Fig. 2a) because methane production (the lowest energy yield process) begins at low sulfate concentrations (Martens and Berner, 1974). The low values of $\delta^{13}C_{CH_4}$ in the methanogenesis zone are typical due to the large carbon isotope fractionation that occurs during methane production, thereby leaving the methane that is produced isotopically light and the DIC isotopically heavy. Dissolved organic carbon increased and sulfate concentration decreased, which could create an opportunity for a shift in the dominant microorganisms.

The highest bacterial diversity was found in the methanogenesis zone (6–9 cm). Comparisons of sequences from previous studies (Nüsslein et al., 2001; Schwarz et al., 2007a) to those in our study showed low similarity. Moreover, this level of similarity was also the lowest (52 %) compared to the other depths we sampled. *Proteobacteria* and *Chloroflexi* percentages increased at this depth. *Deltaproteobacteria* sequences from this depth were remotely related to those of the upper part of the sediment. Even though *Deltaproteobacteria* are best known for their sulfate reduction metabolism, they can shift their metabolism in response to depleted sulfate concentrations (Plugge et al., 2011).

BGD
11, 9813–9852, 2014

At the sediment depth of 6–9 cm, archaeal similarity (cut-off 90 %) to previous studies was 31 %. The earlier studies on microbial communities in LK (Nüsslein et al., 2001; Schwarz et al., 2007a) showed that about 60 % of the detected archaeal 16S rRNA genes sequences could be linked to the known process of hydrogenotrophic methanogensis (methane production from H_2 and CO_2) dominated by the family *Methanomicrobiaceae* and 15–22 % were affiliated with acetoclastic methanogenesis (methane production from acetate) dominated by *Methanosaetaceae* (Schwarz et al., 2007b). Both of those families belong to the *Methanomicrobia*.

In our clone libraries the class *Methanomicrobia* was represented by only small percentage in the upper part of the sediment (0–3 cm) (Fig. 4b), which could indicate the methanogenesis activity of other microbial populations. *Thermoplasmata* and MBG-D of the *Euryarchaeota* at this depth were also classified in our library. *Thermoplasmata* exploit a wide range of habitats, from soil and lake sediment (Teske and Sørensen, 2008) to bovine rumen (Poulsen et al., 2013), and that class contains a clade of methylotrophic methanogens found in the bovine rumen, which may indicate that *Thermoplasmata* can function as methanogens in diverse environments. The characteristics of *Thermoplasmata* and MBG-D as novel methanogens may contribute to the methane production in the top (0–15 cm) part of the sediment. Moreover, their ability to utilize the methanogenic metabolic pathway indicates they may be among the archaea capable of AOM via reverse methanogensis (Hallam et al., 2004).

Below the maximum methane production zone (around 20 cm), methane concentrations began to decrease while $\delta^{13}C_{CH_4}$ values increased (Fig. 2a), an outcome that may be due to the AOM process, which leaves residual methane isotopically heavier. Depleted $\delta^{13}C_{TLE}$ (Fig. 2d) in the deep part of the sediment also supports the presence of AOM with the production of light biomass from methane oxidation. In addition, although all the suitable electron acceptors at this depth were depleted, both Fe(II) and Mn(II) increased (Fig. 2b). Also, $\delta^{56}Fe$ values (Fig. 2d) of dissolved iron in the deep sediment were isotopically negative, similar to sediments with active dissimilatory bacterial iron reduction (Severmann et al., 2006) and are an indication of active

BGD
11, 9813–9852, 2014

iron reduction in the deep sediments and not just diffusion. The increase in Fe(II) concentrations below a depth of 15 cm was probably supported by the absence of sulfide. The potential of highly reactive Fe(III) oxides to drive AOM in LK was also supported by our set of mesocosm incubation studies (Sivan et al., 2011). Since manganese oxide concentrations were very low (~ 0.04 %) throughout the LK sediment column (Serruya et al., 1974), iron oxide seemed to play a bigger role in this AOM process.

A few possible mechanisms for the finding of AOM in the deep part of the sediment can be suggested based on the geochemical profiles and the microbial communities (as explained below). A possible direct process could be through new, currently unknown bacteria/archaea that reduce iron and utilize methane. Possible indirect processes include: (1) reduction of Fe(III) by sulfide to elemental sulfur and other sulfur intermediates, which produces sulfate (disproportionation) for sulfate driven AOM (such as in Holmkvist et al., 2011). (2) Reduction of Fe(III) by utilizing H_2 (Lovley, 1991), which creates a low concentration of H_2 and drives "reverse methanogenesis(Hallam et al., 2004)" by the archaea in the deep sediment. (3) An aerobic methane oxidation pathway in an anaerobic environment as described by Ettwig et al. (2010), utilizing methane while using iron oxides to generate the oxygen needed to oxidize the methane.

In the deep methanotrophic zone (sample from 29–32 cm), bacterial diversity was lower than in the methanogenesis zone but higher than in the upper layer (6–9 cm) of the sediment. At 68 %, bacterial similarity (cut-off 90 %) to previous studies was the highest. The changes in bacterial diversity with depth could be related to the availability of different electron acceptors and of organic matter (Nam et al., 2008). In the deep sediment *Proteobacteria* and *Chloroflexi* have the highest percentages (Fig. 3b). Our sequences of *Proteobacteria* and *Nitrospirae* phyla were the bacterial candidates for a direct mechanism of iron reduction in a consortia with archaea (e.g., ANME) or for indirect mechanisms of disproportionation or "reverse methanogenesis". *Deltaproteobacteria* is one of the main candidate of AOM via iron reduction (Niemann and Elvert, 2008), because of their presence in the ANME consortium that performs AOM via sulfate reduction. Sequences of the SVa485 order *(Deltaproteobacteria*) (Fig. 4a)

BGD
11, 9813–9852, 2014

from the bottom part of the sediment were similar to those found in different aquatic environments, but the metabolic functions of members of this order are not clear. *Pelobacter carbinolious* (Lovley et al., 1995), a member of SVa485 capable of Fe(III) and sulfur reduction, had a high similarity (> 90 %) to a few of the SVa485 sequences in our samples. Additionally, the presence of the *Deltaproteobacteria* at the deepest sediment depth sampled and the observed accumulation of acetate with depth (acetate increases with depth to 5 µM at around 30 cm; Adler et al., unpublished) could indicate their exploitation of a different metabolic path in the deep sediment than in the upper part of the sediment.

Another hypothesized participant in direct/indirect AOM via iron reduction belongs to the *Nitrospirae* phylum, which increased with depth (from no detection in the upper part to 11 % in the sample from 29–32 cm). Schwarz et al. (2007b) showed by SIP-RNA not only that *Nitrospirae* was present, but also that it was functionally bioactive. Although *Nitrospirae* is a known nitrate oxidizer (Ehrich et al., 1995), the conditions of this environment suggest that it utilized another metabolic pathway. *Nitrospirae* also include the iron reducing candidates *Magnetobacterium bavaricum* (Spring et al., 1993) and sulfur reducers (Sonne-Hansen and Ahring, 1999). The aligned reference sequence (Fig. 4a) shows that iron reduction could be the main mechanism in that environment, a hint that this clade may be responsible for the iron reduction in the deep LK sediment.

The finding that our *Gammaprotobacteia* sequences were similar (> 90 %) to *Methylocaldum szegediense* (Bodrossy et al., 1997), an aerobic methanotrophic bacteria (Fig. 4a), was an indication of the possible existence of the third indirect mechanism of anaerobic methane oxidation via an oxygenic pathway. In addition to this aerobic methanotrophic bacterium, our archaeal sequences in the deep sediment were affiliated with ammonia oxygenating archaea (see below), which also indicated an oxygenic pathway in this anaerobic zone.

In the bottom part of the sediment the similarity (cut-off 90 %) of the archaeal sequences to those in previous studies was the lowest (18 %). Moreover, 16S rRNA sequences affiliated with *Thaumarchaeota* were at the highest percentage. The ob-

BGD
11, 9813–9852, 2014

served increase in *Thaumarchaeota* may indicate the significance in the sediment of this novel phylum, which comprises not only all known archaeal ammonia oxidizers, but also several clusters of environmental sequences representing microorganisms with unknown energy metabolisms (Pester et al., 2011). The main known characteristic of *Thaumarchaeota* is the enzyme ammonia monooxygenase, which belongs to the enzyme family of copper containing membrane bound monooxgenases that possess wide substrate ranges. Closely related enzymes, which can often perform the same function but with different substrates, include ammonia oxidizing bacteria with ammonia (in *Gammaproteobacteria*) and methane as a substitute (Lontoh et al., 2000). However, a microorganism's metabolic energy is mainly defined by its downstream enzyme machinery (Tavormina et al., 2011). Members of *Thaumarchaeota* phylum could have enzymes that are able to capture methane due to the enzymes' phylogenetic proximities to methane monooxgenases, but that activity requires the necessary downstream metabolic pathway, which, if they have that ability, renders them good candidates for group of methanotrophic archaea. This indirect pathway can be similar to that found in the NC10 phylum (Zhu et al., 2012), which produces oxygen via the reduction of nitrite and the oxidation of methane, but with iron oxides.

The Miscellaneous Crenarchaeotic Group (MCG) is a cosmopolitan class (Fig. 4b) assigned to the *Thaumarchaeota* phylum whose members are found mostly in anoxic habitats and have the capability to take up organic carbon (Biddle et al., 2006). Because of their huge environmental range and their complex phylogeny, the MCG collectively possess great metabolic diversity(Jiang et al., 2008). Current evidence for members of the MCG lineage suggests that they may obtain energy from the anaerobic oxidation of methane, but they do so via a dissimilatory methane-oxidizing process and they do not assimilate its carbon (Biddle et al., 2006). Our own sequences (Fig. 5b) were very similar (> 96 %) to the reference sequences from those types of environments. Therefore, the MCG may also be responsible for the unknown microorganism with a direct mechanism for methane oxidation in the LK profile.

BGD
11, 9813–9852, 2014

The *Euryarchaeota* phylum has diverse metabolic mechanisms in various environments. The sequences affiliated to our clone library (Fig. 5b) show that methanogenesis could be one of the mechanisms functioning in the deep sediment. Those archaea could perform "reverse methanogenesis" while bacterial iron reducers utilize the H_2 produced, which drives this mechanism.

To summarize, this study attempted to correlate between geochemical and microbial profiles in lake sediments. Geochemical and microbial analyses of the deep sediment of LK were performed. The geochemical data suggest three main zones of electron acceptor activities: sulfate reduction, methanogenesis and a novel, deep iron-driven AOM. The prokaryotic analysis provided clues about the microorganisms that are involved in this novel process and the metabolic paths that occur throughout the microbial assemblage. For AOM via iron reduction to occur, a number of potential pathways and their combinations have been suggested. Phyla that become enriched (*Thaumarchaeota*, *Proteobacteria* and *Nitrospirae)* with depth can be assumed to participate in the AOM process either directly or indirectly. A possible direct process could be through new, currently unknown bacteria/archaea that reduce iron and utilize methane, which may be carried out by a MCG as a methanotroph in consortium with an iron reducer like *Nitrospirae*. Possible indirect processes could be Fe(III) reduction by sulfide, oxidation of the sulfide to elemental sulfur and other sulfur intermediates and then disproportionation to sulfide and sulfate and sulfate driven AOM (such as in (Holmkvist et al., 2011)). It could be also reduction of Fe(III) by utilizing H_2, which creates a low concentration of H_2 and drives "reverse methanogenesis". This could occur by *Nitrospirae* and/or *Deltaproteobacteria*. Both *Nitrospirae* and/or *Deltaproteobacteria* could reduce the iron while in a consortium with methanogenic MBG-D or reduce the iron with sulfur minerals to create sulfate that *Deltaproteobacteria* could utilize while in a consortium with a MCG as a methanotrophic archaea. Anaerobic oxidation of the methane coupled to nitrite reduction pathway as described by Ettwig et al. (2010) could occur by *Thaumarchaeota* with a monooxygenase enzyme that can utilize methane while using iron oxides to generate the oxygen needed to oxidize the methane.

BGD
11, 9813–9852, 2014

Our findings suggest these possible mechanisms in the deep part of LK sediment. However, further research involving a larger sample of the microbial community and characterization of the relevant functional genes will provide better indications as to the compositions of the microbial communities at the different depths. Lab experiments to identify the microorganisms involved in this novel process by enrichment and cultivation by slurry incubation together with geochemical analyses will improve our understanding of the specific mechanism of AOM via iron reduction. Together a better understanding of the biogeochemical makeup of this sediment and of the microbial communities that drive it will be achieved.

The Supplement related to this article is available online at doi:10.5194/bgd-11-9813-2014-supplement.

Acknowledgements. We would like first to thank to the anonymous reviewers for their thorough reviews that improved the ms significantly. We thank M. Adler for her assistance in the field and in the laboratory. Thanks to the members of Orit's and Ariel's laboratories for all the help. Thanks to N. Paramasivam for his help in cloning. Many thanks to V. Orphan, S. Connon and K. Dawson from Caltech for their help with the ARB program and for their fruitful discussions. This research was funded by the Water Authority of Israel (O.S. and W.E.).

References

Adler, M., Eckert, W., and Sivan, O.: Quantifying rates of methanogenesis and methanotrophy in Lake Kinneret sediments (Israel) using pore-water profiles, Limnol. Oceanogr., 56, 1525–1535, 2011.

Beal, E. J., House, C. H., and Orphan, V. J.: Manganese- and iron-dependent marine methane oxidation, Science, 325, 184–187, 2009.

Ben-Dov, E., Shapiro, O. H., Siboni, N., and Kushmaro, A.: Advantage of using inosine at the 3' termini of 16S rRNA gene universal primers for the study of microbial diversity, Appl. Environ. Microb., 72, 6902–6906, 2006.

BGD
11, 9813–9852, 2014

Biddle, J. F., Lipp, J. S., Lever, M. a, Lloyd, K. G., Sørensen, K. B., Anderson, R., Fredricks, H. F., Elvert, M., Kelly, T. J., Schrag, D. P., Sogin, M. L., Brenchley, J. E., Teske, A., House, C. H., and Hinrichs, K.-U.: Heterotrophic Archaea dominate sedimentary subsurface ecosystems off Peru, P. Natl. Acad. Sci. USA, 103, 3846–3851, 2006.

Bligh, E. G. and Dyer, W. J.: A rapid method of total lipid extraction and purification, Can. J. Biochem. Phys., 37, 911–917, 1959.

Bodrossy, L., Holmes, E. M., Holmes, A. J., Kovács, K. L., and Murrell, J. C.: Analysis of 16S rRNA and methane monooxygenase gene sequences reveals a novel group of thermotolerant, Arch. Microbiol., 168, 493–503, 1997.

Boetius, A., Ravenschlag, K., Schubert, C. J., Rickert, D., Widdel, F., Gieseke, A., Amann, R., Jørgensen, B. B., Witte, U., and Pfannkuche, O.: A marine microbial consortium apparently mediating anaerobic oxidation of methane, Nature, 407, 623–626, 2000.

Borowski, W. S., Cagatay, N., Ternois, Y., and Paull, C. K.: Data report: carbon isotopic composition of dissolved CO_2, CO_2 gas, and methane, Blake-Bahama Ridge and northeast Bermuda Rise, ODP Leg 172, Proc. Ocean Drill. Program, Sci. Results, 172, 1–16, 2000.

Borrel, G., Lehours, A.-C., Crouzet, O., Jézéquel, D., Rockne, K., Kulczak, A., Duffaud, E., Joblin, K., and Fonty, G.: Stratification of Archaea in the deep sediments of a freshwater meromictic lake: vertical shift from methanogenic to uncultured archaeal lineages., PLoS One, 7, e43346, doi:10.1371/journal.pone.0043346, 2012.

Borrok, D. M., Wanty, R. B., Ridley, W. I., Wolf, R., Lamothe, P. J., and Adams, M.: Separation of copper, iron, and zinc from complex aqueous solutions for isotopic measurement, Chem. Geol., 242, 400–414, 2007.

Butler, I. B., Archer, C., Vance, D., Oldroyd, A., and Rickard, D.: Fe isotope fractionation on FeS formation in ambient aqueous solution, Earth Planet. Sc. Lett., 236, 430–442, 2005.

Chao, A.: Nonparametric estimation of the number of classes in a population, Scand. J. Stat., 11, 265–270, 1984.

Chao, B. Y. A. and Ma, M.: Stopping rules and estimation for recapture debugging with unequal failure rates, Biometrika, 80, 193–201, 1993.

Chistoserdova, L., Vorholt, J. A., and Lidstrom, M. E.: A genomic view of methane oxidation by aerobic bacteria and anaerobic archaea, Genome Biol., 6, 208.1–208.6, 2005.

Cline, J. D.: Spectrophotometric determination of hydrogen sulfide In natural waters, Limnol. Oceanogr., 14, 454–458, 1969.

BGD
11, 9813–9852, 2014

Colwell, R. K., Chao, A., Gotelli, N. J., Lin, S.-Y., Mao, C. X., Chazdon, R. L., and Longino, J. T.: Models and estimators linking individual-based and sample-based rarefaction, extrapolation and comparison of assemblages, J. Plant Ecol.-UK, 5, 3–21, 2012.

Cottrell, M. T. and Kirchman, D. L.: Natural assemblages of marine proteobacteria and members of the cytophaga-flavobacter cluster consuming low- and high-molecular-weight dissolved organic matter, Appl. Environ. Microb., 66, 1692–1697, 2000.

DeLong, E. F.: Archaea in coastal marine environments., P. Natl. Acad. Sci. USA, 89, 5685–5689, 1992.

Eckert, T.: The Influence of Chemical Stratification in the Water Column on Sulfur and Iron Dynamics in Pore Waters and Sediments of Lake Kinneret, Israel, M.Sc. thesis, University of Bayreuth, Germany, 2000.

Eckert, W. and Conrad, R.: Sulfide and methane evolution in the hypolimnion of a subtropical lake: a three-year study, Biogeochemistry, 82, 67–76, 2007.

Eckert, W., Imberger, J., and Saggio, A.: Biogeochemical response to physical forcing in the water column of a warm monomictic lake, Biogeochemistry, 61, 291–307, 2002.

Ehrich, S., Behrens, D., Lebedeva, E., Ludwig, W., and Bock, E.: A new obligately chemolithoautotrophic, nitrite-oxidizing bacterium, *Nitrospira moscoviensis* sp. nov., and its phylogenetic relationship, Arch. Microbiol., 164, 16–23, 1995.

Ettwig, K. F., Van Alen, T., van de Pas-Schoonen, K. T., Jetten, M. S. M., and Strous, M.: Enrichment and molecular detection of denitrifying methanotrophic bacteria of the NC10 phylum, Appl. Environ. Microb., 75, 3656–3662, 2009.

Ettwig, K. F., Butler, M. K., Le Paslier, D., Pelletier, E., Mangenot, S., Kuypers, M. M. M., Schreiber, F., Dutilh, B. E., Zedelius, J., and de Beer, D.: Nitrite-driven anaerobic methane oxidation by oxygenic bacteria, Nature, 464, 543–548, 2010.

Froelich, P. N., Klinkhammer, G. P., Bender, M. L., Luedtke, N. A., Heath, G. R., Cullen, D., Dauphin, P., Hammond, D., Hartman, B., and Maynard, V.: Early oxidation of organic matter in pelagic sediments of the eastern equatorial Atlantic: suboxic diagenesis, Geochim. Cosmochim. Ac., 43, 1075–1090, 1979.

Good, I. J.: The population frequencies of species and the estimation of population parameters, Biometrika, 40, 237–264, 1953.

Hadas, O. and Pinkas, R.: Sulfte-reduction process in sediments of Lake Kinneret, Israel, Hydrobiologia, 235, 295–301, 1992.

BGD
11, 9813–9852, 2014

Hallam, S. J., Putnam, N., Preston, C. M., Detter, J. C., Rokhsar, D., Richardson, P. M., and DeLong, E. F.: Reverse methanogenesis: testing the hypothesis with environmental genomics, Science, 305, 1457–1462, 2004.
Hansel, C. M., Fendorf, S., Jardine, P. M., and Francis, C. A.: Changes in bacterial and archaeal community structure and functional diversity along a geochemically variable soil profile, Appl. Environ. Microb., 74, 1620–1633, 2008.
Hinrichs, K. U., Hayes, J. M., Sylva, S. P., Brewer, P. G., and DeLong, E. F.: Methane-consuming archaebacteria in marine sediments, Nature, 398, 802–805, 1999.
Holler, T., Wegener, G., Knittel, K., Boetius, A., Brunner, B., Kuypers, M. M. M., and Widdel, F.: Substantial 13C/12C and D/H fractionation during anaerobic oxidation of methane by marine consortia enriched in vitro, Environ. Microbiol. Rep., 1, 370–376, 2009.
Holmkvist, L., Ferdelman, T. G., and Jørgensen, B. B.: A cryptic sulfur cycle driven by iron in the methane zone of marine sediment (Aarhus Bay, Denmark), Geochim. Cosmochim. Ac., 75, 3581–3599, 2011.
Huber, T., Faulkner, G., and Hugenholtz, P.: Bellerophon: a program to detect chimeric sequences in multiple sequence alignments, Bioinformatics, 20, 2317–2319, 2004.
Jiang, H., Dong, H., Yu, B., Ye, Q., Shen, J., Rowe, H., and Zhang, C.: Dominance of putative marine benthic Archaea in Qinghai Lake, north-western China., Environ. Microbiol., 10, 2355–2367, 2008.
John, S. G. and Adkins, J. F.: Analysis of dissolved iron isotopes in seawater, Mar. Chem., 119, 65–76, 2010.
Kinnaman, F. S., Valentine, D. L., and Tyler, S. C.: Carbon and hydrogen isotope fractionation associated with the aerobic microbial oxidation of methane, ethane, propane and butane, Geochim. Cosmochim. Ac., 71, 271–283, 2007.
Knittel, K. and Boetius, A.: Anaerobic oxidation of methane: progress with an unknown process., Annu. Rev. Microbiol., 63, 311–334, 2009.
Lehours, A.-C., Evans, P., Bardot, C., Joblin, K., and Gérard, F.: Phylogenetic diversity of archaea and bacteria in the anoxic zone of a meromictic lake (Lake Pavin, France), Appl. Environ. Microb., 73, 2016–2019, 2007.
Lloyd, K. G., Schreiber, L., Petersen, D. G., Kjeldsen, K. U., Lever, M. a., Steen, A. D., Stepanauskas, R., Richter, M., Kleindienst, S., Lenk, S., Schramm, A., and Jørgensen, B. B.: Predominant archaea in marine sediments degrade detrital proteins, Nature, 496, 215–218, 2013.

BGD
11, 9813–9852, 2014

Lontoh, S., DiSpirito, A. A., Krema, C. L., Whittaker, M. R., Hooper, A. B., and Semrau, J. D.: Differential inhibition in vivo of ammonia monooxygenase, soluble methane monooxygenase and membrane-associated methane monooxygenase by phenylacetylene., Environ. Microbiol., 2, 485–494, 2000.
Lovley, D. R.: Dissimilatory Fe(III) and Mn(IV) reduction., Microbiol. Rev., 55, 259–287, 1991.
Lovley, D. R. and Klug, M. J.: Sulfate reducers can outcompete methanogens at concentrations sulfate reducers can outcompete methanogens sulfate concentrationst at freshwater, Appl. Environ. Microb., 45, 187–192, 1983.
Lovley, D. R., Phillips, E. J. P., Lonergan, D. J., and Widman, P. K.: Fe(III) and S0 reduction by Pelobacter carbinolicus, Appl. Environ. Microb., 61, 2132–2138, 1995.
Ludwig, W., Strunk, O., Westram, R., Richter, L., Meier, H., Yadhukumar, Buchner, A., Lai, T., Steppi, S., Jobb, G., Förster, W., Brettske, I., Gerber, S., Ginhart, A. W., Gross, O., Grumann, S., Hermann, S., Jost, R., König, A., Liss, T., Lüssmann, R., May, M., Nonhoff, B., Reichel, B., Strehlow, R., Stamatakis, A., Stuckmann, N., Vilbig, A., Lenke, M., Ludwig, T., Bode, A., and Schleifer, K.-H.: ARB: a software environment for sequence data, Nucleic Acids Res., 32, 1363–1371, 2004.
Magurran, A. E. (Ed.): Ecological Diversity and Its Measurement, Princeton University Press, Princeton, 1988.
Martens, C. S. and Berner, R. A.: Methane production in the interstitial waters of sulfate-depleted marine sediments, Science, 185, 1167–1169, 1974.
Milucka, J., Ferdelman, T. G., Polerecky, L., Franzke, D., Wegener, G., Schmid, M., Lieberwirth, I., Wagner, M., Widdel, F., and Kuypers, M. M. M.: Zero-valent sulphur is a key intermediate in marine methane oxidation, Nature, 491, 541–546, 2012.
Miyashita, A., Mochimaru, H., Kazama, H., Ohashi, A., Yamaguchi, T., Nunoura, T., Horikoshi, K., Takai, K., and Imachi, H.: Development of 16S rRNA gene-targeted primers for detection of archaeal anaerobic methanotrophs (ANMEs), FEMS Microbiol. Lett., 297, 31–37, 2009.
Nam, Y.-D., Sung, Y., Chang, H.-W., Roh, S. W., Kim, K.-H., Rhee, S.-K., Kim, J.-C., Kim, J.-Y., Yoon, J.-H., and Bae, J.-W.: Characterization of the depth-related changes in the microbial communities in Lake Hovsgol sediment by 16S rRNA gene-based approaches, J. Microbiol., 46, 125–136, 2008.

BGD
11, 9813–9852, 2014

Niemann, H. and Elvert, M.: Diagnostic lipid biomarker and stable carbon isotope signatures of microbial communities mediating the anaerobic oxidation of methane with sulphate, Org. Geochem., 39, 1668–1677, 2008.
Niemann, H., Lösekann, T., de Beer, D., Elvert, M., Nadalig, T., Knittel, K., Amann, R., Sauter, E. J., Schlüter, M., and Klages, M.: Novel microbial communities of the Haakon Mosby mud volcano and their role as a methane sink, Nature, 443, 854–858, 2006.
Nüsslein, B., Chin, K. J., Eckert, W., and Conrad, R.: Evidence for anaerobic syntrophic acetate oxidation during methane production in the profundal sediment of subtropical Lake Kinneret (Israel), Environ. Microbiol., 3, 460–470, 2001.
Nüsslein, B., Eckert, W., and Conrad, R.: Stable isotope biogeochemistry of methane formation in profundal sediments of Lake Kinneret (Israel), Limnol. Oceanogr., 48, 1439–1446, 2003.
Orphan, V. J., House, C. H., Hinrichs, K. U., McKeegan, K. D., and DeLong, E. F.: Methane-consuming archaea revealed by directly coupled isotopic and phylogenetic analysis, Science, 293, 484–487, 2001.
Orphan, V. J., House, C. H., Hinrichs, K. U., McKeegan, K. D., and DeLong, E. F.: Multiple archaeal groups mediate methane oxidation in anoxic cold seep sediments, P. Natl. Acad. Sci. USA, 99, 7663–7668, 2002.
Pester, M., Schleper, C., and Wagner, M.: The Thaumarchaeota: an emerging view of their phylogeny and ecophysiology, Curr. Opin. Microbiol., 14, 300–306, 2011.
Plugge, C. M., Zhang, W., Scholten, J. C. M., and Stams, A. J. M.: Metabolic flexibility of sulfate-reducing bacteria, Front. Microbiol., 2, 1–8, 2011.
Poulsen, M., Schwab, C., Borg Jensen, B., Engberg, R. M., Spang, A., Canibe, N., Højberg, O., Milinovich, G., Fragner, L., Schleper, C., Weckwerth, W., Lund, P., Schramm, A., and Urich, T.: Methylotrophic methanogenic Thermoplasmata implicated in reduced methane emissions from bovine rumen, Nat. Commun., 4, 1–7, 2013.
Pruesse, E., Peplies, J., and Glöckner, F. O.: SINA: accurate high-throughput multiple sequence alignment of ribosomal RNA genes, Bioinformatics, 28, 1823–1829, 2012.
Raghoebarsing, A. A., Pol, A., Van de Pas-Schoonen, K. T., Smolders, A. J. P., Ettwig, K. F., Rijpstra, W. I. C., Schouten, S., Damsté, J. S. S., den Camp, H. J. M. O., and Jetten, M. S. M.: A microbial consortium couples anaerobic methane oxidation to denitrification, Nature, 440, 918–921, 2006.

BGD
11, 9813–9852, 2014

Schloss, P. D. and Handelsman, J.: Introducing DOTUR, a computer program for defining operational taxonomic units and estimating species richness, Appl. Environ. Microb., 71, 1501–1506, 2005.
Schoell, M.: Multiple origins of methane in the earth, Chem. Geol., 71, 1–10, 1988.
Schubert, C. J., Vazquez, F., Lösekann-Behrens, T., Knittel, K., Tonolla, M., and Boetius, A.: Evidence for anaerobic oxidation of methane in sediments of a freshwater system (Lago di Cadagno), FEMS Microbiol. Ecol., 76, 26–38, 2011.
Schwarz, J. I. K., Eckert, W., and Conrad, R.: Community structure of Archaea and Bacteria in a profundal lake sediment Lake Kinneret (Israel), Syst. Appl. Microbiol., 30, 239–254, 2007a.
Schwarz, J. I. K., Lueders, T., Eckert, W., and Conrad, R.: Identification of acetate-utilizing Bacteria and Archaea in methanogenic profundal sediments of Lake Kinneret (Israel) by stable isotope probing of rRNA, Environ. Microbiol., 9, 223–237, 2007b.
Serruya, C.: Lake Kinneret: the nutrient chemistry of the sediments, Limnol. Oceanogr., 16, 510–521, 1971.
Serruya, C.: Lake Kinneret, 1st edn., Dr. W. Junk, London, 1978.
Serruya, C., Edelstein, M., Pollingher, U., and Serruya, S.: Lake Kinneret sediments: nutrient composition of the pore water and mud water exchanges, Limnol. Oceanogr., 19, 489–508, 1974.
Severmann, S., Johnson, C. M., Beard, B. L., and McManus, J.: The effect of early diagenesis on the Fe isotope compositions of porewaters and authigenic minerals in continental margin sediments, Geochim. Cosmochim. Ac., 70, 2006–2022, 2006.
Siboni, N., Ben-Dov, E., Sivan, A., and Kushmaro, A.: Global distribution and diversity of coral-associated Archaea and their possible role in the coral holobiont nitrogen cycle, Environ. Microbiol., 10, 2979–2990, 2008.
Sivan, O., Adler, M., Pearson, A., Gelman, F., Bar-Or, I., John, S. G., and Eckert, W.: Geochemical evidence for iron-mediated anaerobic oxidation of methane, Limnol. Oceanogr., 56, 1536–1544, 2011.
Smith, P. F., Langworthy, T. A., and Smith, M. R.: Polypeptide nature of growth requirement in yeast extract for thermoplasma polypeptide nature of growth requirement in yeast extract for thermoplasma acidophilum, J. Bacteriol., 124, 884–892, 1975.
Sonne-Hansen, J. and Ahring, B. K.: *Thermodesulfobacterium hveragerdense* sp. nov., and *Thermodesulfovibrio islandicus* sp. nov., two thermophilic sulfate reducing bacteria isolated from a Icelandic hot spring, Syst. Appl. Microbiol., 22, 559–564, 1999.

BGD
11, 9813–9852, 2014

Spring, S., Amann, R., Ludwig, W., Schleifer, K. H., van Gemerden, H., and Petersen, N.: Dominating role of an unusual magnetotactic bacterium in the microaerobic zone of a freshwater sediment., Appl. Environ. Microb., 59, 2397–2403, 1993.
Stahl, D. A. and Amann, R.: Development and application of nucleic acid probes in bacterial systematics, in: Nucleic Acid Techniques in Bacterial Systematics, John Wiley & Sons Ltd., Chichester, England, 205–248, 1991.
Stookey, L. L.: Ferrozine – a new spectrophotometric reagent for iron, Anal. Chem., 42, 779–781, 1970.
Tamaki, H., Sekiguchi, Y., Hanada, S., Nomura, N., Matsumura, M., Nakamura, K., and Kamagata, Y.: Comparative analysis of bacterial diversity in freshwater sediment of a shallow eutrophic lake by molecular and improved cultivation-based techniques comparative analysis of bacterial diversity in freshwater sediment of a shallow eutrophic lake by molecul, Appl. Environ. Microb., 71, 2162–2169, 2005.
Tamura, K., Peterson, D., Peterson, N., Stecher, G., Nei, M., and Kumar, S.: MEGA5: molecular evolutionary genetics analysis using maximum likelihood, evolutionary distance, and maximum parsimony methods, Mol. Biol. Evol., 28, 2731–2739, 2011.
Tavormina, P. L., Orphan, V. J., Kalyuzhnaya, M. G., Jetten, M. S. M., and Klotz, M. G.: A novel family of functional operons encoding methane/ammonia monooxygenase-related proteins in gammaproteobacterial methanotrophs, Environ. Microbiol. Rep., 3, 91–100, 2011.
Teske, A. and Sørensen, K. B.: Uncultured archaea in deep marine subsurface sediments: have we caught them all?, ISME J., 2, 3–18, 2008.
Thauer, R. K.: Functionalization of methane in anaerobic microorganisms, Angew. Chem. Int. Edit., 49, 6712–6713, 2010.
Valentine, D. L.: Biogeochemistry and microbial ecology of methane oxidation in anoxic environments: a review, Anton. Leeuw. Int. J. G., 81, 271–282, 2002.
Whiticar, M. J.: Carbon and hydrogen isotope systematics of bacterial formation and oxidation of methane, Chem. Geol., 161, 291–314, 1999.
Wobus, A., Bleul, C., Maassen, S., Scheerer, C., Schuppler, M., Jacobs, E., and Röske, I.: Microbial diversity and functional characterization of sediments from reservoirs of different trophic state, FEMS Microbiol. Ecol., 46, 331–347, 2003.
Yamada, T. and Sekiguchi, Y.: Cultivation of uncultured chloroflexi subphyla: significance and ecophysiology of formerly uncultured chloroflexi "Subphylum I" with natural and biotechnological relevance, Microbes Environ., 24, 205–216, 2009.

BGD
11, 9813–9852, 2014

Yamada, T., Sekiguchi, Y., Hanada, S., Imachi, H., Ohashi, A., Harada, H., and Kamagata, Y.: *Anaerolinea thermolimosa* sp. nov., *Levilinea saccharolytica* gen. nov., sp. nov., and *Leptolinea tardivitalis* gen. nov., sp. nov., novel filamentous anaerobes, and description of the new classes *Anaerolineae classis* nov., and *Caldilineae classis* nov. in the, Int. J. Syst. Evol. Micr., 56, 1331–1340, 2006.

Zheng, Y., Hou, L., Newell, S., Liu, M., Zhou, J., Zhao, H., You, L., and Cheng, X.: Community dynamics and activity of ammonia-oxidizing prokaryotes in intertidal sediments of the yangtze estuary., Appl. Environ. Microb., 80, 408–419, 2014.

Zhu, B., van Dijk, G., Fritz, C., Smolders, A. J. P., Pol, A., Jetten, M. S. M., and Ettwig, K. F.: Anaerobic oxidization of methane in a minerotrophic peatland: enrichment of nitrite-dependent methane-oxidizing bacteria, Appl. Environ. Microb., 78, 8657–8665, 2012.

BGD
11, 9813–9852, 2014

Table 1. Bacterial sequence distributions using different richness and diversity indexes.

Depth	No. of clones sequenced	No. of OTUs (97 %)	Chao value (min/max)	Ace value (min/max)	Shannon index (min/max)	Coverage (%)
Bac-1 (0–3 cm)	32	26	68 (39.74–154.37)	79.76 (43.1–195.02)	3.19 (2.93–3.45)	34.38
Bac-3 (6–9 cm)	57	53	461.33 (201.25–1177.68)	574.902 (246.41–1719.86)	3.94 (3.74–4.13)	12.28
Bac-11 (29–32 cm)	38	33	134.5 (68.14–326.17)	162.5 (74.64–435.74)	3.44 (3.2–3.68)	23.68

BGD
11, 9813–9852, 2014

Table 2. Archaeal sequence distributions using different richness and diversity indexes.

Depth	No. of clones sequenced	No. of OTUs (97 %)	Chao value (min/max)	Ace value (min/max)	Shannon index (min/max)	Coverage (%)
Arch-1 (0–3 cm)	46	27	46.13 (33.16–86.41)	54.53 (42.72–75.21)	2.97 (2.66–3.28)	60.87
Arch-3 (6–9 cm)	52	28	53.5 (36.05–108.79)	60.64 (39.75–118.65)	3.09 (2.85–3.33)	65.38
Arch-11 (29–32 cm)	55	30	43.6 (34.29–73.09)	54.79 (39.16–97.06)	3.19 (2.97–3.42)	69.09

BGD
11, 9813–9852, 2014

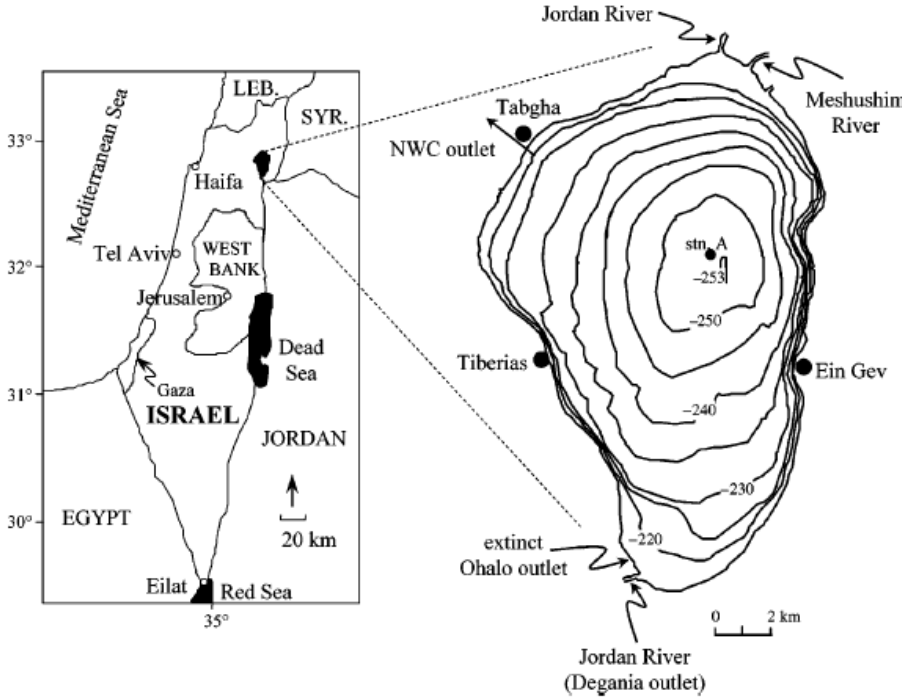

Figure 1. Schematic location of Lake Kinneret. Numbers correspond to altitude measured in meters from the level of Lake Kinneret. Cores were taken from station A (taken from Hambright et al., 2004).

BGD
11, 9813–9852, 2014

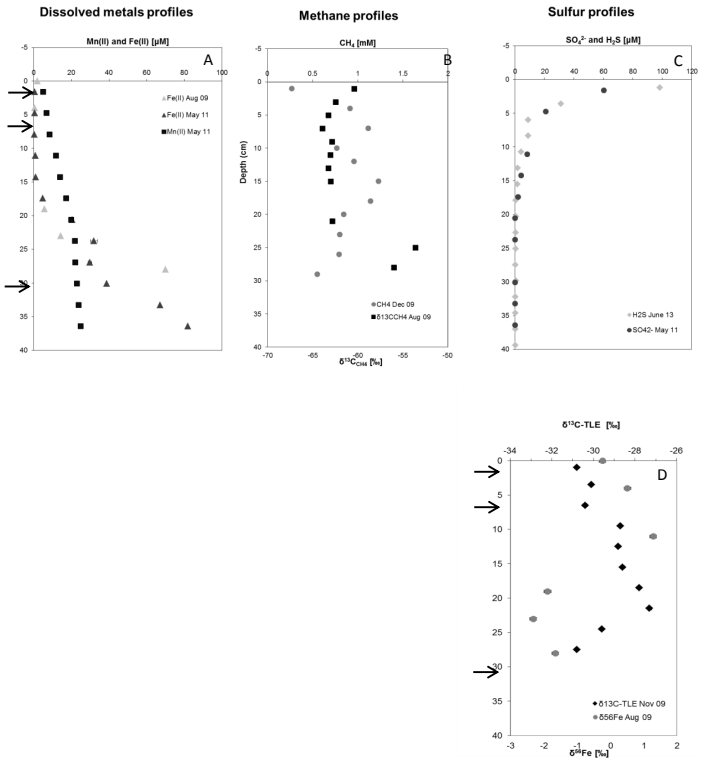

Figure 2. Geochemical porewater profiles in LK sediment. **(A)** Headspace measurements of methane (gray circles) and $\delta^{13}C_{CH_4}$ (black squares) in the sediments, **(B)** electron acceptor profiles of dissolved Fe(II) (gray triangles) and Mn (II) (black squares) in the porewater, **(C)** profile of SO_4^{-2} (black circles) and sulfide (gray diamonds) in the porewater, **(D)** $\delta^{13}C$ of total lipids extraction (TLE) (black diamonds) from the sediment, and $\delta^{56}Fe$ (gray circles) of the dissolved iron in the porewater. Black arrows indicate the sampled sections for 16S rRNA gene analysis.

BGD
11, 9813–9852, 2014

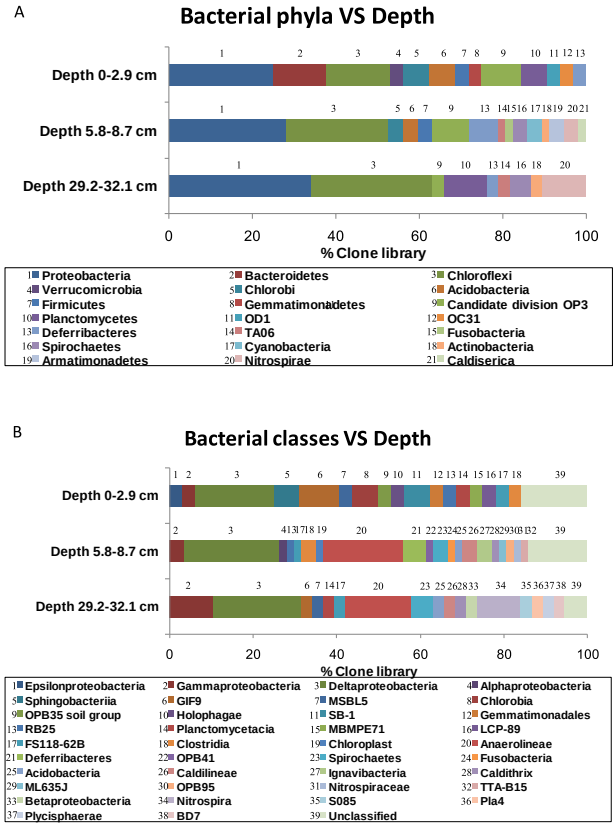

Figure 3. Classification of bacterial sequences using the SINA program. **(A)** Phyla distribution of sequences of the clone libraries at the different depths. **(B)** Class distributions of sequences of the clone libraries at the different depths. Note: unclassified sequences were classified by manual alignment with the ARB program.

BGD
11, 9813–9852, 2014

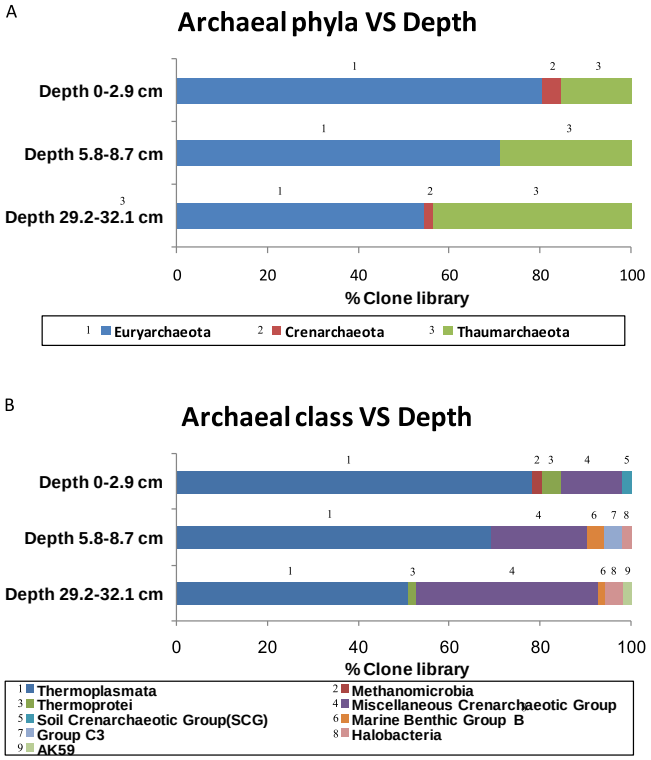

Figure 4. Classification of archaeal sequences using the SINA program. **(A)** Phyla distributions of sequences of the clone libraries at the different depths. **(B)** Class distributions of sequences of the clone libraries at the different depths. Note: unclassified sequences were classified by manual alignment with the ARB program.

BGD
11, 9813–9852, 2014

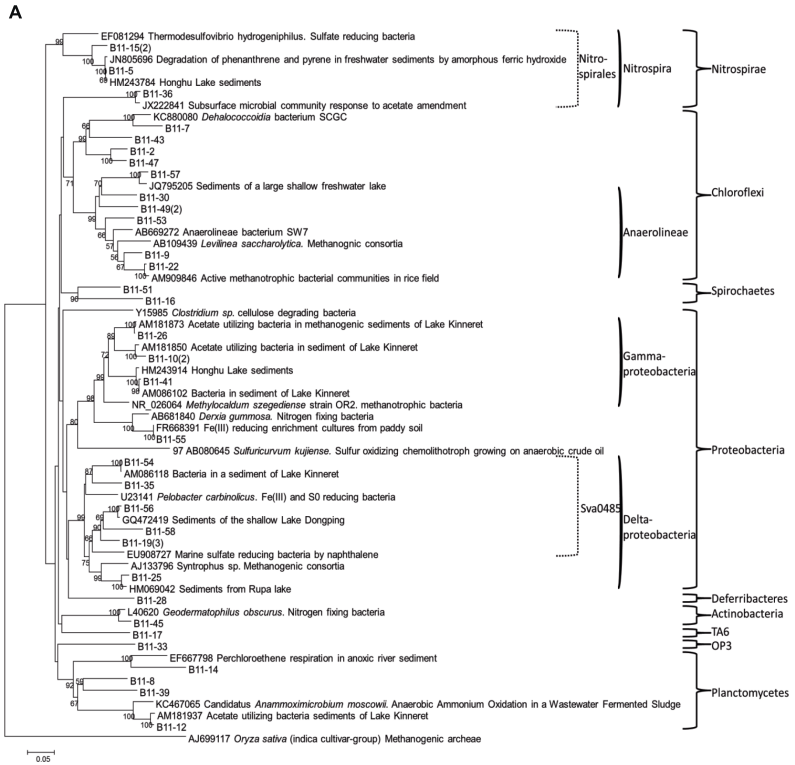

Figure 5a. Neighbor joining phylogenetic tree from the bottom part of the core showing the affiliation of 16S rRNA gene OTUs. **(A)** Bacterial phylogenetic tree. Bootstrap values greater than 50 % of 1000 resampling are shown near nodes. The brackets near the sequence number indicate the number of sequences represented by this OTU. The SINA classification is shown by brackets: the braces represent the phylum, the thick black brackets represent the class, the dashed brackets represent the order and the normal brackets represent the family. Bar = 5 % estimated sequence divergence.

BGD
11, 9813–9852, 2014

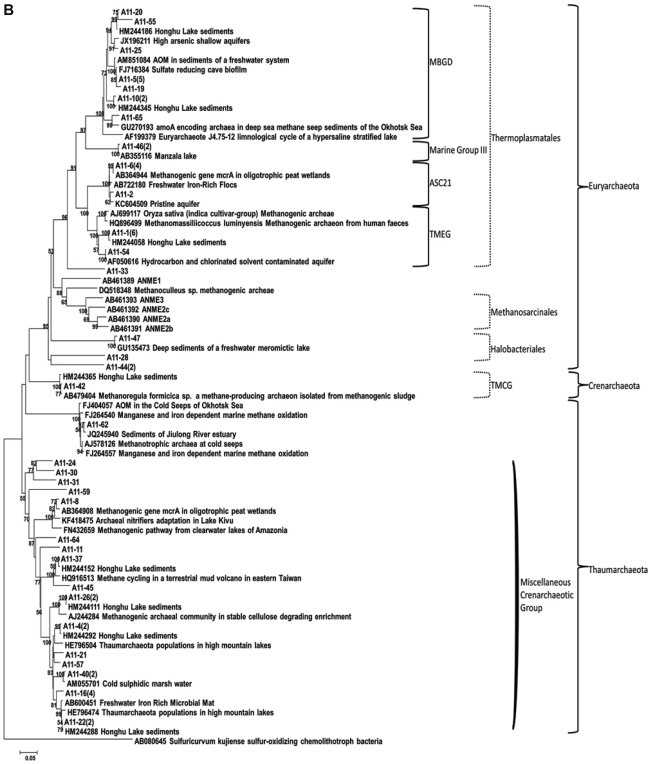

Figure 5b. Neighbor joining phylogenetic tree from the bottom part of the core showing the affiliation of 16S rRNA gene OTUs. **(B)** Archaeal phylogenetic tree. Bootstrap values greater than 50 % of 1000 resampling are shown near nodes. The brackets near the sequence number indicate the number of sequences represented by this OTU. The SINA classification is shown by brackets: the braces represent the phylum, the thick black brackets represent the class, the dashed brackets represent the order and the normal brackets represent the family. Bar = 5 % estimated sequence divergence.

BGD
11, 9813–9852, 2014